

Rates of formation and dissipation of clumping reveal lagged responses in tropical tree populations

MATTEO DETTO^{1,2} AND HELENE C. MULLER-LANDAU¹

¹Smithsonian Tropical Research Institute, Apartado 0843-03092, Balboa, Panama

Abstract. The dynamics of spatial patterns of plant populations can provide important information about underlying processes, yet they have received relatively little attention to date. Here we investigate the rates of formation and dissipation of clusters and the relationship of these rates to the degree of aggregation (clumping) in models and in empirical data for tropical trees. In univariate models, exact solutions and simulations show that the rate of change of spatial patterns has a specific, linear relationship to the degree of aggregation at all scales. Shorter dispersal and/or weaker negative density dependence (NDD) result in both denser and longer-lasting clusters. In multivariate host-parasite models in contrast, the rate of change of spatial pattern is faster relative to the level of aggregation. We then analyzed the dynamics of spatial patterns of stems ≥ 1 cm diameter in 221 tropical tree species from seven censuses spanning 28 yr. We found that for most species, the rates of change in spatial patterns were faster than predicted from univariate models given their aggregation. This indicates that more complex dynamics involving multivariate interactions induce time lags in responses to aggregation in these species. Such lags could arise, for example, if it takes time for natural enemies to locate aggregations of their hosts. This combination of theoretical and empirical results thus shows that complex multilevel models are needed to capture spatiotemporal dynamics of tropical forests and provides new insights into the processes structuring tropical plant communities.

Key words: aggregation; dispersal limitation; host-parasite dynamic; local interactions; Lotka-Volterra systems; moment equations; negative density dependence; scale dependent analysis; spatial persistence.

INTRODUCTION

In sessile organisms such as plants, local dispersal and local competitive interactions commonly result in the formation of distinct spatial patterns, which evolve in characteristic ways over time. Spatially explicit theory can help us to understand how spatial patterns and their temporal dynamics depend upon dispersal, competition, and other processes, and thereby enable us to use spatiotemporal analyses to glean the maximum possible insights into underlying processes. A fundamental question for any population is whether population dynamics are governed primarily by intraspecific interactions, or whether interspecific interactions also contribute importantly. For example, suppose that the dynamics of a species in a diverse community is completely described by its dispersal ability and interactions among conspecifics. Density-dependent conspecific interactions may phenomenologically represent a multitude of underlying mechanisms, including intraspecific competition for resources and apparent competition due to natural enemies (Holt 1977). The expectation of this model would be that the *spatiotemporal dynamic* of that

species (the formation and dissipation of clusters due to recruitment and mortality), would be completely predictable (in a statistical sense) from the initial spatial distribution and the demographic turnover rate alone. However, in more complex models involving two or more interacting species, knowledge of the spatial pattern of one species would rarely suffice to predict its dynamics.

Among tropical trees, local dispersal and local interactions are pervasive and of known importance for population spatial patterns (Muller-Landau et al. 2002, Uriarte et al. 2005, Seidler and Plotkin 2006). Extensive interspecific variation in aggregation is explained in part by species dispersal mode (Seidler and Plotkin 2006, Harrison et al. 2013). And many studies have found that establishment, growth, and survival are negatively influenced by local conspecific density (e.g., Harms et al. 2000, Comita et al. 2010). Experimental studies show that these negative conspecific effects can be attributed in large part to soil biota, in particular fungal pathogens (Mangan et al. 2010, Bagchi et al. 2014). Although there are other important factors that shape the distribution of individuals including habitat association (Harms et al. 2001, Baldeck et al. 2013) and clustered disturbances (Manrubia and Solé 1997), existing evidence suggests these act mainly at scales > 100 m (Condit et al. 2013, Detto et al. 2013). Local

Manuscript received 13 August 2015; accepted 5 November 2015; final version received 13 December 2015. Corresponding Editor: D. B. Metcalfe.

²E-mail: dettom@si.edu

dispersal and interactions are the main mechanisms of pattern formation at spatial scales <100 m, the scales that can be analyzed in typical large (10–60 ha) forest plots with high statistical confidence.

Local interactions are often analyzed and modeled simply in terms of conspecific negative density-dependence (Comita et al. 2010, Detto and Muller-Landau 2013, Lebrija-Trejos et al. 2014). However, this univariate approximation of what are fundamentally multivariate interactions with natural enemies or competitors may fail to capture important aspects of the spatiotemporal dynamics. The approximation of these multivariate interactions as conspecific NDD is appealing and at least partially successful because natural enemy effects are stronger where conspecific density is higher. Insofar as this assumption is adequate, we should be able to make reliable predictions about the evolution of spatial patterns based on current spatial distribution and demographic turnover. In contrast, if the rate at which clusters expand or contract is substantially faster or slower than expected under the simplified assumptions that all relevant information is contained in the current distribution of conspecifics, this would provide an indication of the importance of other influences (e.g., natural enemies or competing species) or more complex interactions among individuals of that species (e.g., adult-juvenile competition) that induce time lags. In this case, more detailed models of the interactions involved would be required to capture the dynamics of spatial arrangements.

We can test the presence of lagged responses through analyses of multitemporal mapped plant data as illustrated in Fig. 1. The availability of mapped plant data for large forest dynamic plots (Losos and Leigh 2004, Anderson-Teixeira et al. 2014) has stimulated a large body of spatial analyses based on point process theory (Wiegand and Moloney 2013). However, spatiotemporal dynamics in plant species are still relatively little investigated and poorly understood, despite the fact that robust inferences about ecological processes require knowledge of how patterns change over time (Law et al. 2009). One important spatiotemporal property is how long spatial patterns remain coherent or persist before they are dissipated by competition, pest pressure, treefalls, or stochastic drift, a property we call *spatial persistence*. We measure this by analyzing the correlation of spatial patterns measured at different times, and how this correlation decays as the time interval increases. From a practical point of view, our measure of persistence can be thought of as the minimum census interval after which two maps of individuals can be considered statistically independent at a specific spatial scale (Fig. 1). This property is closely related to the concept of population synchrony in metapopulations, that is, the correlation of fluctuations in population densities among different communities (Lande et al. 1999). Synchrony strongly influences regional population dynamics (Allen et al., 1993), slows the spread of an invasion, prolongs time to extinction, and facilitates

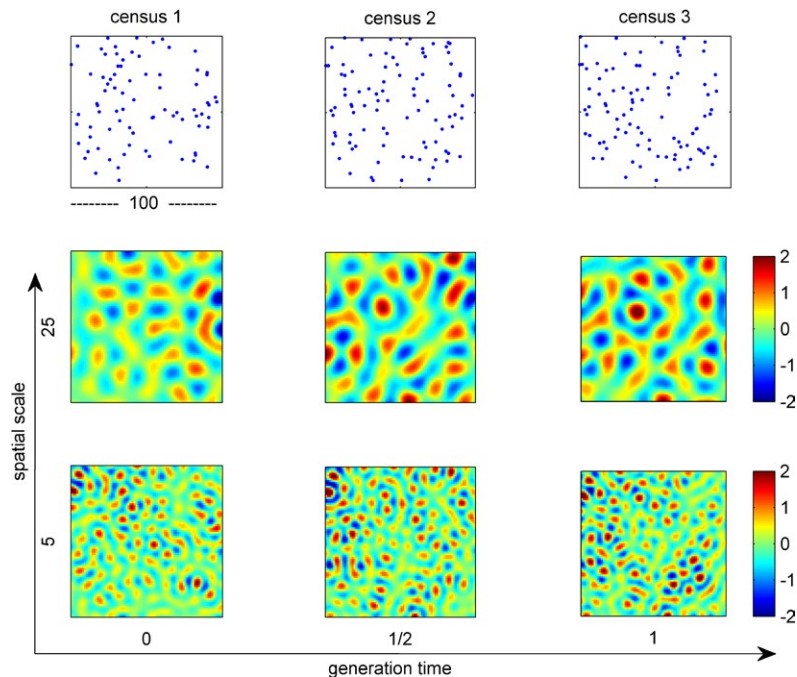


FIG. 1. (Top) Spatiotemporal dynamics of a point process representing a plant population with local dispersal and local interactions. The process is censused at regular time intervals, with three time points depicted here (left to right). The central and bottom panels depict how spatial patterns at two different scales (sampled with a suitable wavelet function) change over time. Red/blue areas indicate high/low degree of clumping at a particular scale.

stable coexistence of a host and parasite (Tilman et al. 1994, Ovaskainen and Cornell 2006a). In continuous spatially explicit models (sensu Bolker and Pacala 1997), this property assumes even more relevance, because the scales are represented on a continuous axis, allowing for more complex interplay among spatial processes.

The expected rate of change of spatial pattern of a population in a homogeneous environment has been described using solutions of individual-based population models in which spatial patterns arise from local dispersal and local interactions (Bolker and Pacala 1997, Law and Dieckmann 2000, Ovaskainen and Cornell 2006b). Although extremely simplified, these models can help us to identify basic properties which can be used as benchmarks when analyzing empirical data. In such models, different combinations of dispersal and interaction parameters can produce a wide variety of spatial patterns (Bolker et al. 2000) consistent with observed patterns from a large tropical forest plot (Detto and Muller-Landau 2013). In general, local dispersal produces aggregation (in space), and clusters persist because new individuals recruit disproportionately near existing individuals. In contrast, NDD inhibits the production, establishment or survival of new individuals close to conspecifics, facilitating the quick dissipation of dense clumps. Here we specifically use such models to investigate the persistence of spatial patterns, a previously unexplored property, and its relationship to aggregation.

Empirical studies of spatial patterns are often concerned with understanding interspecific variation and its relationship to species abundances and traits (e.g., Condit et al. 2000, Seidler and Plotkin 2006). In order to make meaningful comparisons among species with different abundance, aggregation metrics are usually normalized by the number of individuals (Daley and Vere-Jones 2003). In particular, metrics are commonly chosen so that they show no trend with abundance if all species followed a null model of complete spatial randomness. However, this criterion alone does not insure that there are no systematic trends with abundance under alternative (non-null) models in which spatial patterns are driven by local dispersal or other processes with identical parameters across abundances. For example, Condit et al. (2000) and Gilbert et al. (2010) used normalized circle statistics to analyze spatial patterns in tropical and temperate forests, respectively, finding that regular patterns are infrequent and rare species are more aggregated by these metrics. Interpretation of this and similar findings requires understanding how metrics are related to abundance under process-based models of spatial patterns.

In this study, we combine theoretical and empirical findings to gain insights into the processes driving spatiotemporal dynamics in tropical forests. Using asymptotic solutions and simulations of spatially explicit, individual-based population models, we first establish theoretical relationships of aggregation and spatial persistence to dispersal, local interactions, and abundance for a univariate (single species) system and a two-variable

(host-parasite) system. We then quantified aggregation and persistence for 221 species sampled in the Barro Colorado Island 50 ha forest dynamics plot in seven censuses spanning almost 30 yr, related these to abundance, and interpreted these patterns in light of the theory. Results suggest that complex multilevel interactions induce a lagged response in spatiotemporal dynamics of tropical forests, allowing conspecifics to form clusters that expand and contract at faster rates than expected under the hypothesis of simple conspecific NDD.

THEORY

Spatiotemporal point process and second order moments

Consider a spatiotemporal point process that generates a pattern of $n(t)$ points representing live individuals in a bounded area (e.g., Fig. 1). At each time t , a realization of this process can be represented as the sum of Dirac δ -functions centered at the $n(t)$ point locations $\mathbf{x}_i = (x_i, y_i)$ and zero everywhere else:

$$p(\mathbf{x}, t) = \sum_{i=1}^{n(t)} \delta(\mathbf{x} - \mathbf{x}_i).$$

The second-order moment is defined as the covariance of the function $p(\mathbf{x}, t)$ between two locations \mathbf{x} and \mathbf{x}' and two times t and $t + \tau$

$$M(\mathbf{x}, \mathbf{x}', t, t + \tau) = E [p(\mathbf{x}, t)p(\mathbf{x}', t + \tau)]$$

where the expectation is taken over all possible realizations of the process (Daley and Vere-Jones 2003). The function M describes how a dynamical process covaries in both space and time. For homogeneous and isotropic conditions the function M depends only on the difference

$$r = |\mathbf{x}' - \mathbf{x}|: M(\mathbf{x}, \mathbf{x}', t, t + \tau) = g(r, t, \tau).$$

The extension to the multivariate case is used to describe how spatial patterns change for two locally interacting groups of individuals, i and j (species, size classes, functional types etc.) and is defined as

$$M_{ij}(\mathbf{x}, \mathbf{x}', t, t + \tau) = E [p_i(\mathbf{x}, t)p_j(\mathbf{x}', t + \tau)].$$

For example, it describes how segregation persists for one species relative to another in communities with resource competition. Note that the multivariate second moment is generally asymmetric:

$$M_{ij}(\mathbf{x}, \mathbf{x}', t, t + \tau) \neq M_{ji}(\mathbf{x}, \mathbf{x}', t, t + \tau) \quad \tau \neq 0, i \neq j.$$

The covariance function is often given in spectral form in the Fourier domain (Bartlett 1964, Bolker and Pacala 1997, Detto and Muller-Landau 2013). As we work with radially symmetric functions, the Fourier transform simplifies into the Hankel transform

$$\tilde{g}(\omega, t, \tau) = \int g(r, t, \tau) J_0(\omega r) r dr$$

where J_0 is a Bessel function of the first kind (following standard notation, throughout this paper the Fourier transform of a function is denoted by a tilde (\sim) and *spatial frequency* by ω).

Spatially explicit, individual-based models: univariate models (single species)

Spatially explicit ecological models express dispersal and local interactions with kernel functions, $D(L_D)$ and $C(L_C)$, where L_D and L_C are the dispersal and interaction distances (Bolker and Pacala 1997). Ovaskainen and Cornell (2006a,b) derived linearized equations for the dynamics of $\tilde{g}(\omega, t, \tau)$ for a spatial single-species model:

$$\frac{d\tilde{g}(\omega, t, 0)}{dt} = 2\tilde{w}(\omega, t)\tilde{g}(\omega, t, 0) + v(t) \quad (1a)$$

$$\frac{d\tilde{g}(\omega, t, \tau)}{d\tau} = \tilde{w}(\omega, t + \tau)\tilde{g}(\omega, t, \tau) \quad (1b)$$

where the source term $v(t)$ is the scale-independent noise variance, which includes both fecundity and mortality stochasticity, and the function $\tilde{w}(\omega, t)$ expresses the rate at which spatial variability is produced or dissipated. Eq. 1a describes how the second spatial moment $\tilde{g}(\omega, t, 0)$ varies with time as new individuals recruit and others die. Eq. 1b describes how the covariance between two spatial distributions, sampled at different time, varies as function of the time interval.

There are several ways local density dependence can be incorporated in spatial logistic models. These can be divided into pre- and post-dispersal. Pre-dispersal density dependence occurs when the production of fruits or seeds is influenced by the presence of neighboring plants. Post-dispersal density dependence may affect either the establishment of offspring or their survival throughout their various stages of life. We focus first on models with density dependence in the establishment of offspring because, as shown later, these are the only nontrivial cases that are analytically tractable.

This model satisfies Eqs 1a and 1b in the asymptotic limits where L_D and/or L_C are infinitely large (Appendix S1). The asymptotic cases correspond to (1) a spatially random model of births and deaths ($L_C = \infty, L_D = \infty$), henceforth the “nonspatial model”; (2) a “local dispersal” model where individuals are displaced from parents according to a dispersal kernel, but establishment is independent of local conspecific density ($L_C = \infty$); and (3) a “local NDD” model in which establishment depends on local density but dispersal is global ($L_D = \infty$). Mean densities for these three cases converge to the classic logistic equation.

We derive the analytical solutions for the steady-state of Eq. 1a, that is, $\tilde{g}(\omega, t = \infty, \tau = 0) = \tilde{g}^*(\omega, 0)$ (Appendix S1):

$$\frac{\tilde{g}^*(\omega, 0)}{N} = \begin{cases} [1 - \tilde{D}(\omega)]^{-1} & L_C \rightarrow \infty & \text{local dispersal} \\ 1 & L_C \rightarrow \infty, L_D \rightarrow \infty & \text{nonspatial} \\ [1 + \phi \tilde{C}(\omega)]^{-1} & L_D \rightarrow \infty & \text{local NDD} \end{cases} \quad (2)$$

Where ϕ , is the odds ratio of the failure to establish (the probability of failing to establish divided by the probability of successfully establishing) and N the equilibrium

population density. Thus, as expected, the nonspatial case with infinite dispersal and interaction range has no spatial structure; the local dispersal case with global interaction has spatial structure dependent exclusively on the dispersal kernel $\tilde{D}(\omega)$; and the local competition case with infinite dispersal has spatial structure dependent on the competition kernel, $\tilde{C}(\omega)$ and interaction strength ϕ . Note that these solutions are independent of the generation time ($1/r_0$).

It follows from Eq. 1b that the decay of the spatiotemporal correlation is in general a non-separable exponential function of time lag τ :

$$\frac{\tilde{g}^*(\omega, \tau)}{\tilde{g}^*(\omega, 0)} = \begin{cases} e^{-[1 - \tilde{D}(\omega)] r_0 \tau} & L_C \rightarrow \infty & \text{local dispersal} \\ e^{-r_0 \tau} & L_C \rightarrow \infty, L_D \rightarrow \infty & \text{nonspatial} \\ e^{-[1 + \phi \tilde{C}(\omega)] r_0 \tau} & L_D \rightarrow \infty & \text{local NDD} \end{cases} \quad (3)$$

For linearized systems, i.e., systems where the second order dynamics can be expressed as ordinary linear differential equations (as in Eq. 1a), the rate of change of spatial pattern at a particular scale s is equal to the individual turnover rate:

$$\tilde{g}^*(s, 0) \tilde{w}(s) = N r_0 \quad (4)$$

where the scale is defined as the inverse of the frequency $s = 2\pi \omega^{-1}$. This then implies a perfect equivalence between aggregation and persistence, i.e., $\frac{\tilde{g}^*(s, 0)}{N} = \frac{r_0}{\tilde{w}(s)}$.

We refer to $\log(\tilde{g}^*(s, 0)/N)$ as the aggregation and to $\log(r_0/\tilde{w}(s))$ as the persistence of spatial pattern at scale s (or simply persistence). Note that this measure of aggregation is normalized to abundance, and this measure of persistence is normalized to the demographic turnover rate and thus $\log(r_0/\tilde{w}(s))$ is a measure of the persistence of structures at scale s relative to the persistence of individuals.

Multivariate models (multilevel interactions)

The single species model generalizes to a multivariate model, e.g., of interspecific resource competition or host-parasite dynamics (Law and Dieckmann 2000). It is convenient to introduce matrix notation for this multivariate case. Let m be the number of variables. In the $m = 2$ case, these matrices are

$$\tilde{G}(\omega, t, \tau) = \begin{bmatrix} \tilde{g}_{11}(\omega, t, \tau) & \tilde{g}_{12}(\omega, t, \tau) \\ \tilde{g}_{21}(\omega, t, \tau) & \tilde{g}_{22}(\omega, t, \tau) \end{bmatrix}, \quad \tilde{W}(\omega, t) = \begin{bmatrix} \tilde{w}_{11}(\omega, t, \tau) & \tilde{w}_{12}(\omega, t, \tau) \\ \tilde{w}_{21}(\omega, t, \tau) & \tilde{w}_{22}(\omega, t, \tau) \end{bmatrix}, \quad V(t) = \begin{bmatrix} v_{11}(t) & v_{12}(t) \\ v_{21}(t) & v_{22}(t) \end{bmatrix}$$

and the corresponding linearized equations are

$$\frac{d\tilde{G}(\omega, t, 0)}{dt} = \tilde{W}(\omega, t) \tilde{G}(\omega, t, 0) + [\tilde{W}(\omega, t) \tilde{G}(\omega, t, 0)]^T + V(t) \quad (5a)$$

$$\frac{d\tilde{G}(\omega, t, \tau)}{d\tau} = \tilde{W}(\omega, t + \tau) \tilde{G}(\omega, t, \tau). \tag{5b}$$

The above set of matrix differential equations is exact when all species have L_D and/or L_c tending to infinity (see Appendix S1 for details). For these cases, mean densities converge to the classic Lotka-Volterra competition equations (Pacala 1997). The solution of the first order differential matrix equation is given in the form

$$\tilde{G}(\omega, t, \tau) = e^{\tilde{W}(\omega, t)\tau} \tilde{G}(\omega, t, 0) \tag{6}$$

which can be analytically evaluated using for example the Putzer’s algorithm. It follows that, even for a linearized case, if the off-diagonal elements of $\tilde{W}(\omega)$ are different from zero (indicating multilevel interactions), the rate of change of spatial pattern of species i can no longer be represented by a single exponential decay, but instead by a more complex dynamic expressed as a combination of several exponential functions.

Further theoretical analysis of this multivariate model is beyond the scope of this study. We explore the spatiotemporal dynamics of these models through a case study involving simulations of a host-parasite model.

METHODS

Analytical solutions and simulations

We sought analytical solutions and conducted simulations to examine aggregation and persistence of spatial structures as a function of spatial scale and temporal lag in the univariate and multivariate model. We specifically examined the spatiotemporal correlation functions and compared analytical solutions to simulation results for the three simplified univariate cases with establishment NDD: global dispersal with local interactions, local dispersal with global interactions, and global dispersal and interactions. We further examined two models with survival NDD where dispersal and local interactions are both acting on similar scales: a single species model with negative density dependent mortality, and a host-parasite model with density-dependent infestation rate.

Simulations were conducted on a square arena (100 × 100 m) with periodic boundaries with constant number of individuals (zero-sum game). At the beginning, N individuals were placed at random. Parents dispersed offspring according to a dispersal kernel D . In the model with conspecific negative density-dependent establishment, the probability to establish depended linearly on local density around the seed according to an interaction kernel C . Once an individual was established, a random individual was killed. For negative density-dependent survival, an individual was killed with probability which depended linearly on local density according to an interaction kernel C . For the host-parasite model, the probability of a host to be attacked was linearly proportional to the presence of parasites in the neighborhood, within a range described by C . Once a host was

attacked and died, the parasite took its place. The host had no mortality other than that caused by the parasite, and parasites had a density-independent death rate. Simulations were conducted for different values of dispersal distance (1–10), interaction range (1–10) and number of individuals (50–1500). For comparison with empirical data, we focused on aggregated cases, largely ignoring disaggregated cases.

Quantification of aggregation and persistence

We quantified spatial aggregation and the persistence of spatial patterns at multiple scales with second order spectral moments estimated using wavelet transforms (Detto and Muller-Landau 2013). Given n maps of individuals sampled at time interval dt , a simple estimator of the spatiotemporal covariance at scale s and temporal lag $k dt$ is given by

$$\hat{g}_{ij}(s, k) = \frac{1}{n-k} \sum_{l=1}^{n-k} \int \tilde{I}_t^{(i)}(\omega) \tilde{I}_{l+k}^{*(j)}(\omega) |\tilde{\psi}_s(\omega)|^2 d\omega$$

$$k = 0, 1, \dots, n-1; s = s_0 2^{(0, 1, \dots, J) dj}$$

where $\tilde{I}^{(i)}(\omega)$ is the Fourier transform of the map of individuals for the species or group i , discretized on a regular grid, and $\tilde{\psi}_s(\omega)$ is a wavelet function associated with the scale s . The scale axis is discretized with 43 scales logarithmically spaced between 2 and 157 m ($s_0 = 2, J = 42, dj = 0.15$). We chose a minimum of 2 m because location random errors and the size of the stems becomes dominant below these scales, and a maximum of 157 m because spatial replication becomes limited above this distance due to edge effects. We evaluated $w(s)$, which represents the rate of decay of the spatial structure with scale s , by fitting an exponential model (in k) to the spatiotemporal correlation function, which is $\hat{g}(s, \tau)$ normalized by its value at lag zero, $\hat{g}(s, 0)$:

$$\frac{\hat{g}(s, k)}{\hat{g}(s, 0)} = e^{w(s)k dt}.$$

We evaluated the rate r_0 in the limit $s \rightarrow 0$, as the value of $w(s)$ at the minimum scale.

Empirical case study of tropical tree species

We analyzed empirical spatiotemporal correlation functions of individual tropical tree species using data from the 50 ha forest dynamics plot on Barro Colorado Island, Panama (BCI). This plot was censused in 1982–1983, 1985, and every 5 yr thereafter (Hubbell et al. 1999). The data include positions (to 0.1 m) and species identity of all live free-standing woody stems with diameter at breast height bigger than 1 cm. We analyzed spatiotemporal data for the 221 tree species having >10 individuals in every census. The focal species vary in abundance (N) over three orders of magnitude, and exhibit a wide variety of different spatial distributions. For each species, we estimated second order spectral moments and calculated aggregation

$\log(\tilde{g}^*(\omega,0)/N)$, spatiotemporal correlation functions $\tilde{g}^*(\omega,\tau)/\tilde{g}^*(\omega,0)$, and persistence $\log(r/\tilde{w}(s))$ for different spatial scales and time lags. We investigated how aggregation and persistence varied across species and scales. We analyzed how aggregation and persistence were related to each other at any given scale using model 2 regression, and how the slope of this relationship varied with the spatial scale. (We used model 2 regression because both persistence and aggregation are subject to estimation error and because there is no a priori causal directionality among the two variables.) We quantified the relationships of scale-specific aggregation and persistence to abundance using Kendall rank correlations.

RESULTS

Theoretical results

The univariate case of local dispersal and long-distance interaction naturally shows aggregation for all scales above a critical scale defined by the dispersal distance, while the case of local interactions and long-distance dispersal shows disaggregation for all scales above a critical scale defined by the interaction range (Fig. 2A). The case with long-distance dispersal and long-distance competition (the random process) divides the space into two regions corresponding to aggregated and disaggregated point patterns (Fig. 2A). These asymptotic states are characterized by different spatial persistence (Fig. 2B). Although all spatiotemporal correlations decline exponentially over time (i.e., are linear on a logarithmic axis), disaggregated distributions decay faster than aggregated ones (Fig. 2B). Again, the random process separates these two behaviors. Spatiotemporal correlations in the

random case decay independently of scale, consistent with the scale-independence property of the Poisson process, and drop below 0.1 within two generation times. In contrast, the local dispersal case loses correlation more slowly at scales larger than dispersal distance (Fig. 2B blue surface). The local NDD case shows the opposite behavior; large structures disappear more quickly than small structures, as shown by a back-folding of the red surface in Fig. 2B. Analytical solutions for these asymptotic cases are exact and reproduce the simulation results well.

Different types of NDD lead to different aggregation patterns. For the case of long dispersal and short-range interaction, a model with pre-dispersal fecundity NDD exhibits behavior identical to a model with no NDD (i.e., $\tilde{g}(s,0) = 1$). In contrast, the model with NDD in mortality has no closed solution for the case of short-range interaction, because local interactions generate higher order terms even under long dispersal. Of course, when interaction distances approach infinity, then the type of NDD ceases to matter, and models of all types of NDD have the same asymptotic solutions (as in Eq. 3).

We used simulations to explore the analytically intractable cases with local dispersal and local interaction for both the univariate model and a host-parasite model. We varied abundance, dispersal and interaction distances among realizations, and thus simulations of each model exhibited a great variety of levels of aggregation and persistence (Fig. 3A–D). Across the diverse simulations of the univariate model, we found that aggregation and persistence were essentially equal to each other at all scales, within the limits of sampling error, as expected (Fig. 3D). Note that simulations sometimes produced disaggregated patterns that are rare

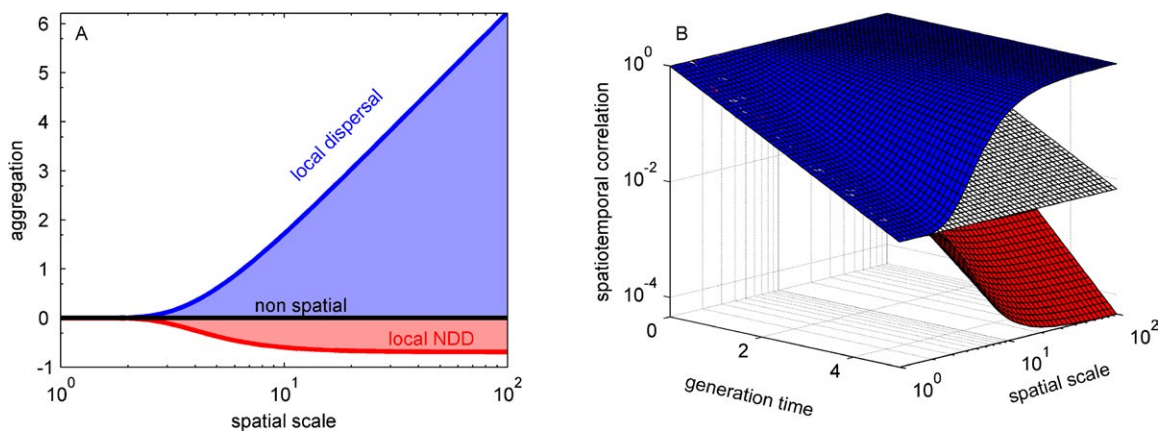


FIG. 2. Exact asymptotic analytical solutions for aggregation (A) and spatiotemporal correlations (B) in a single species population model for three special cases: the nonspatial case with global dispersal and global interaction (black), the local dispersal case with dispersal distance $L_d = 1$ and global interaction (blue), and the local NDD case with global dispersal and interaction range $L_c = 1$ (red). Here aggregation is quantified as the spectral second order moment at time lag zero normalized by abundance, $\log(\tilde{g}^*(\omega,0)/N)$, and the spatiotemporal correlation functions are the second order spectral moment at lag time τ divided by the second order spectral moment at lag time zero $\tilde{g}^*(\omega,\tau)/\tilde{g}^*(\omega,0)$. The black line in A divides the aggregated states (blue shaded area) from the disaggregated states (red shaded area). The black plane in B divides the strongly persistent characteristic of aggregated states (e.g., blue surface) from the weakly persistent characteristic of disaggregated states (e.g., red surface).

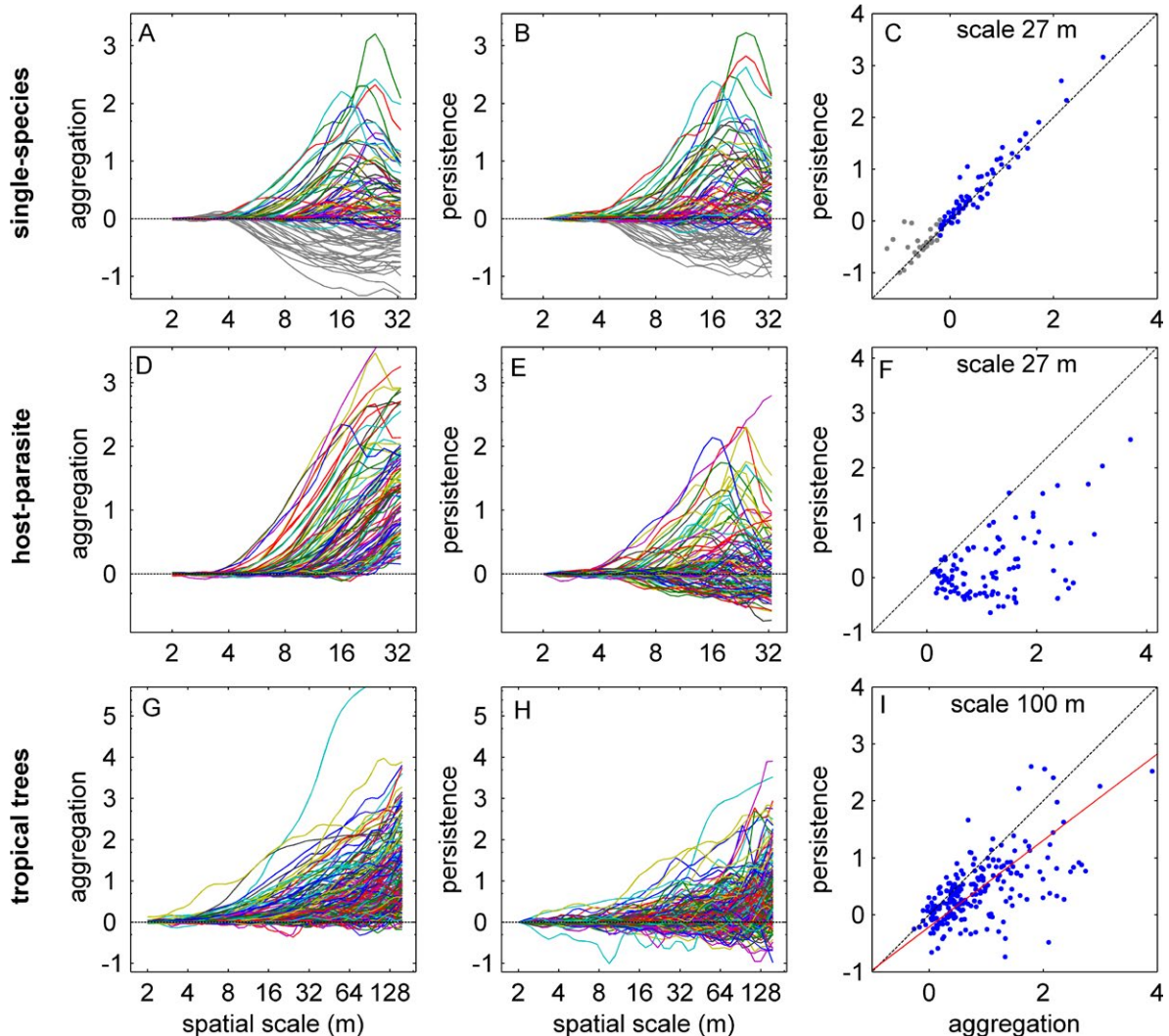


FIG. 3. Aggregation and persistence as a function of spatial scale for simulated single species models with local dispersal and local negative density-dependent mortality (A, B), for the host in simulated host-parasite models with local dispersal and local negative density dependent infestation (D, E), and for 221 tropical tree species on Barro Colorado Island (G, H). For the simulated cases, dispersal distance and interaction range were independently varied between 1 and 10, and population densities between 50 and 1500 (see text for simulation details). Gray lines in (A) and (B) indicate disaggregated distributions which are absent in the empirical data and thus less relevant for comparisons. The relationships between aggregation and persistence at particular spatial scales are shown in (C, F) and (I) respectively for the three cases. The dashed grey lines (C, F, I) indicate the predicted 1:1 relationship between aggregation and persistence for these univariate models, while the red line in I is the reduced major axis relation.

in empirical data (gray lines in Fig. 3A); these nonetheless followed on the same line. (These cases correspond to combinations of large dispersal distances, short interaction ranges and high population densities.) In contrast, simulations of the host-parasite model generally resulted in persistence being lower than aggregation for spatial scales above some threshold determined by model parameters (Fig. 3D–F).

These theoretical findings enable us to make predictions about which species are likely to exhibit more or less persistence in their spatial structures, after accounting for differences in generation time. Species with limited dispersal ability and weak local

interactions are expected to be more aggregated and more spatially persistent than species which are able to disperse longer and/or have stronger negative density dependence. The influences of dispersal on aggregation and persistence are independent of relative abundance. In contrast, the influences of conspecific NDD depend on abundance: common species will be less aggregated and less persistent than rare species having the same dispersal and NDD parameters. Moreover, persistence will be significantly lower than aggregation if the NDD arises from interactions among different systems (e.g., host and parasite). Because of the ways in which spatial patterns

propagate across scales, interspecific variability in functional traits related to dispersal and conspecific NDD (e.g., seed dispersal distance, shade tolerance, pathogen resistance) will generate interspecific variability of aggregation or persistence at scales larger than typical dispersal and interaction distances. At scales smaller than dispersal and interaction distances, however, there will be no significant relationship between species traits and spatiotemporal dynamics.

Empirical results for tropical tree species

Spatiotemporal correlation functions varied among species, as seen in patterns for nine species with different generation times and spatial configurations (Fig. 4). Note that species with long generation times, e.g., *Swartzia simplex*, barely changed from one census to another. In contrast, *Calophyllum longifolium*'s pattern has changed so rapidly that by 2020 it will probably be completely independent from the pattern mapped in 1982. Species with strong dispersal limitation, such as

Rinorea sylvatica and *Anaxagorea panamensis*, showed rapid decay in spatiotemporal correlation at small scales, while at large scales correlations remained quite high. In contrast, the decay in *Guarea bullata* appeared quite uniform across scales.

Overall, persistence was lower than expected under a univariate model given the observed aggregation, especially at larger spatial scales (Fig. 3G–I). For scales of 10 m and higher, aggregation was quite high for most species (Fig. 3G). Ballistically dispersed species such as *A. panamensis* and *R. sylvatica* showed the highest aggregation, confirming the importance of dispersal mechanisms to these patterns. *Hybantus prunifolium*, the most abundant species on the plot, was also highly aggregated. Persistence increased with aggregation among species (Fig. 3I), as predicted by the theory. However, several species showed negative persistence (Fig. 3H), and for scales of 10 m and above, observed persistences were significantly lower than expected based on observed aggregation and the theoretical expectation for univariate systems (Eq. 2, Fig. 3I). This

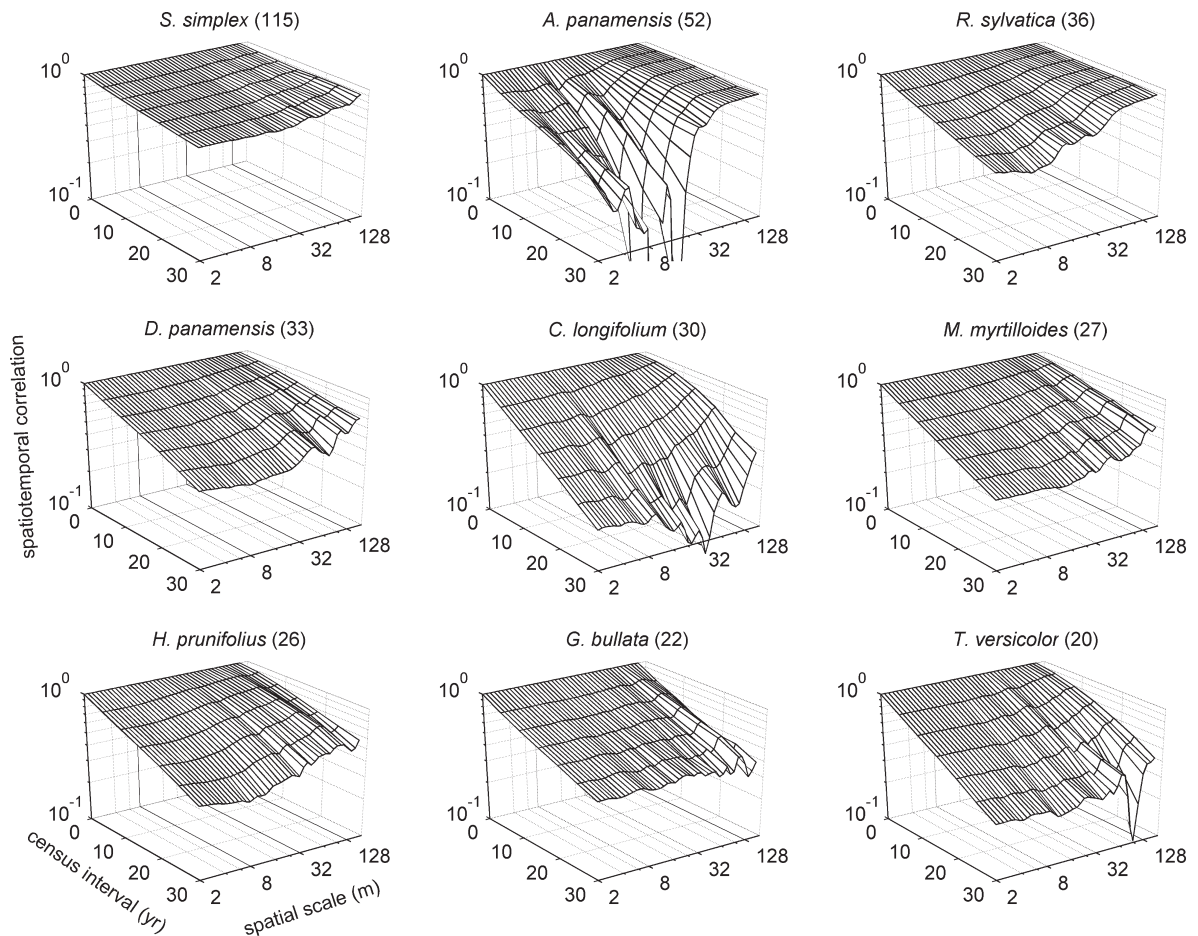


FIG. 4. Examples of spatiotemporal correlation functions, $\tilde{g}^*(s, \tau) / \tilde{g}^*(s, 0)$, for nine tropical tree species censused on BCI during 1982–2010, ordered by decreasing mortality turnover time. The numbers in parentheses indicate the average generation time (yr) base on mortality rates.

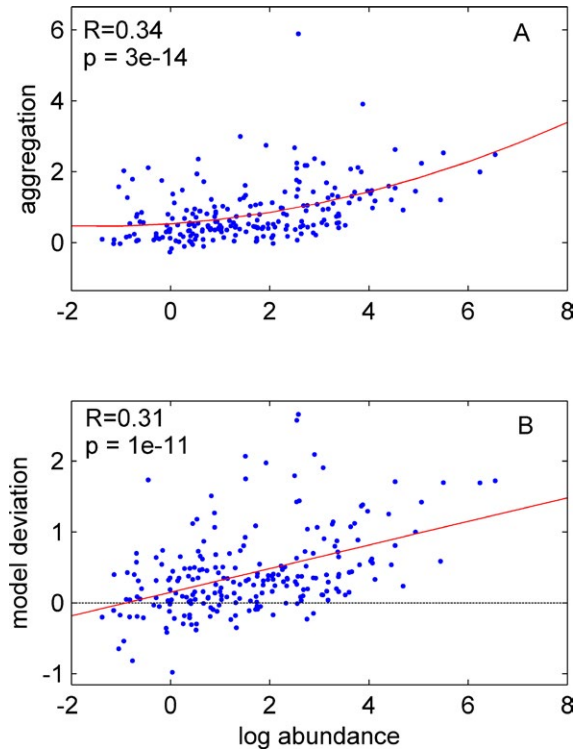


FIG. 5. The empirical relationship of species abundance to aggregation (A), and to aggregation divided by persistence $\log \left[\frac{\hat{g}^*(s,0)}{N} \frac{\hat{w}(s)}{r} \right]$ (B), a measure of deviation from the univariate model prediction, both at the 100 m scale. Best polynomial fits (red lines), Kendall rank correlation coefficients and associated P -values are shown for reference. For results at other scales see Supplementary Material Figure 3.

means that for a given level of aggregation, patterns dissolve more rapidly than expected, or equivalently, that for a given level of persistence aggregation develops more strongly than expected. The departure from the 1:1 line was larger for more aggregated species. Note that for the 10 m scale, persistence was negative (lower than the nonspatial case) for many species, while aggregation was generally positive. Larger departures from theoretical predictions were associated with larger errors in model fit, as evidenced by a positive correlation between the root mean square error of the exponential fit and the ratio between aggregation and persistence (Pearson $R = 0.22$, P value = $7.6e-4$, variables were log transformed).

Abundance was a significant predictor of aggregation and of the deviation of species' persistence-aggregation relationship from that found in univariate models (Fig. 5). Aggregation was significantly positively correlated with abundance across species for scales >10 m, though not for smaller scales (Fig. 5A). The more abundant species also showed larger deviations from the predictions of the univariate model, with higher ratios of aggregation to persistence (Fig. 5B).

DISCUSSION

Theoretical insights

We analyzed spatially explicit, individual-based, plant competition models to show how dispersal limitation and local interactions together influence spatial aggregation and the persistence of spatial structures. Given the complexity of the problem, three asymptotic cases were first introduced to study the effects of dispersal and NDD analytically, but separately, in the univariate model.

Dispersal limitation increases and local NDD decreases the persistence of spatial structures, and these influences are strongly scale-dependent. Spatiotemporal correlations in the nonspatial univariate model decay with a rate determined solely by generation time and independent of scale, as no spatial processes are involved. Local dispersal promotes clustering, and once these structures are formed, new individuals are more likely to be dispersed inside of or in proximity to the cluster, thereby allowing these structures to persist. Thus, in the local dispersal model, spatial structures have longer turnover times than individuals, and turnover times increase with spatial scale. In contrast, local NDD means individuals increasingly fail to establish or survive in crowded areas, thus large clusters disappear more quickly. Spatial structures in the local NDD models have shorter turnover times than individuals, with turnover times decreasing with spatial scale above the range of NDD.

The effects of NDD depend on the life history stage at which it acts, and on whether it is entirely determined by conspecific densities or is dependent on natural enemies that may imperfectly track conspecific densities. NDD can be expressed in fecundity, establishment, or mortality. The asymptotic univariate models in which NDD affects establishment or fecundity are analytically tractable. When NDD affects fecundity (plants in clusters produce fewer viable seeds than plants in isolation), the local NDD case behaves the same as the nonspatial case (supplementary table 1). Basically, long dispersal neutralizes the effect of fecundity NDD on spatial patterns; viable seeds have the same probability to reach any point in space, even areas with high density. In contrast, for local dispersal and local interaction, the pre-dispersal NDD case would be expected to deviate from the nonspatial case. When NDD affects the mortality term, the case with local interactions is not analytically tractable without introducing a closure scheme (Bolker and Pacala 1997), but simulations showed that results are qualitatively similar to those with NDD establishment. In all univariate models, our normalized measure of persistence of spatial patterns was equal to our normalized measure of aggregation at all spatial scales. In contrast, the host-parasite model, with analogous parameter values, produces qualitatively dissimilar results from the univariate models, with persistence significantly lower than aggregation. This behavior is explained by the fact that there is a delay between the buildup of host aggregation and arrival of

the parasite. However, once the parasite reaches an area of high host density (a cluster), its negative influence quickly dissipates the spatial structure.

A key general result is that aggregation is positively correlated with the persistence of spatial structures when spatial pattern is governed by dispersal and NDD, but this correlation becomes weaker in multivariate than in univariate models. This result on the equivalence of persistence and aggregation in univariate models is analytical for the linearized systems treated here, i.e., systems where dynamics at a particular scale are not influenced by and do not influence other scales. Specifically, for a single species model with a given generation time, the rate of dissipation of spatial patterns is inversely proportional to the aggregation level. This establishes a theoretical relationship between aggregation and persistence. This result can be generalized to nonlinear systems, i.e., systems where dispersal and NDD interact simultaneously, as the simulations suggest. This relationship need not hold if the model structure includes time delays either explicitly or implicitly. For example, in models of host-pathogen dynamics it may take time for pathogens to locate and attack aggregations of their hosts, and pathogens may persist in an area for some time after the host aggregation dissipates. Such dynamics effectively lead to time lags in NDD effects and cause aggregated structures to decay faster than they build up. It is important to note that the host-parasite model, here taken as an example, is not the only model that can produce such dynamics. Other models of interacting species, such as colonization-competition trade off models of competitors (Bolker and Pacala 1999), may lead to analogous results.

Empirical insights into tropical trees

Empirical analyses of spatiotemporal patterns in 221 tropical tree species found that persistence was lower than aggregation at larger spatial scales, and that the two were significantly positively correlated at all scales. This relationship was relatively weak at small scales, meaning that spatial structures are formed and dissipated largely independently of the level of aggregation. At these scales interspecific variability in aggregation is minimal, with most species tending to Poisson distributions, and thus this result is not surprising. At large scales, the observed persistence was lower than aggregation. Habitat association cannot explain this pattern, because habitat specialists tend to recruit into the same areas and therefore should have patterns that are more persistent, not less. Furthermore, most of the scales analyzed in this study were smaller than the scales of habitat heterogeneity previously characterized for this study site (Harms et al. 2001).

The pattern of persistence being lower than aggregation in these tropical tree populations can be explained as reflecting a fundamental role for multivariate interactions in the underlying dynamics. Single-species models without time delays cannot adequately reproduce such spatiotemporal dynamics, as persistence always equals aggregation

in such models. Instead, what is required is a multivariate model, such as the host-parasite model we investigated. Interactions between hosts and pathogens, between competing species, or between size or age classes within species produce lagged responses in pattern formations, with consequent build-up of spatiotemporal correlations. In such cases, the single exponential decay model is no longer a correct representation of the dynamics, and a combination of exponential functions with different decay times, as shown in Eq. 7, should be used instead. We noted that in the host-parasite model, disaggregated patterns are more difficult to generate, with the set of parameters we choose, in contrast to the single species model (gray lines in Fig. 3A). This may help to explain why disaggregated patterns are rare in observations.

We found significant positive correlations of species abundance with aggregation. This unexpected result seems at first to disagree with previous findings of a negative correlation between abundance and aggregation (Condit et al. 2000, Flügge et al. 2012), but closer examination of the properties of the relevant statistics shows that these results are entirely compatible, and indeed, expected. In these previous studies, aggregation was measured using a circle statistic, Ω_{0-R} , which can be related to $\tilde{g}(\omega)/N$ by the following equation (in polar coordinates):

$$\begin{aligned} \Omega_{0-R} &= \frac{1}{\pi R^2} \int_0^R \frac{g(\rho) - N\delta(\rho)/\rho}{N^2} 2\pi\rho d\rho \\ &= \frac{1}{NR^2} \int_0^R \int_0^\infty \frac{\tilde{g}(\omega) - N}{N} J_0(\omega\rho)\omega d\omega 2\rho d\rho \\ &= \frac{1}{NR^2} \int_0^\infty \left(\frac{\tilde{g}(\omega)}{N} - 1 \right) J_1(\omega R) 2R d\omega \end{aligned}$$

For a nonspatial Poisson process, both the circle statistic (Ω_{0-R}) and the normalized second order spectral density ($\tilde{g}^*(\omega,0)/N$) we examine take value 1 regardless of species abundance (except $\omega = 4$ where $\tilde{g}(\omega)/N$ has an atomic component). For nonrandom distributions, however, the two indices respond differently to variation in abundance and spatial process parameters by a factor proportional to NR^2 . The relationship of the spectral aggregation measure with underlying process parameters for the three asymptotic cases is given in Eq. 3. These equations show that, when spatial aggregation is driven purely by dispersal, the normalized spectral moment will depend exclusively on the dispersal parameters and be insensitive to abundance. In contrast, given a particular local dispersal distance, the circle statistics will take higher values for rare than for common species, and thus a negative correlation between abundance and circle statistic measures of aggregation is expected if there is no systematic variation in dispersal or NDD with abundance.

The observed increase in our spectral measures of aggregation with abundance suggests that more abundant species have shorter dispersal and/or weaker NDD. If all the species have the same dispersal and same NDD strength (parameter α), our theoretical

analyses predict the opposite pattern, as more abundant species will suffer more from local interactions (for example having a greater odds ratio of the failure to establish, ϕ), and thus will be less aggregated and persistent. The observed increase in aggregation and persistence with abundance can be explained consistently with our theoretical results if more abundant species have shorter dispersal distances or experience weaker conspecific NDD. There is empirical support for both these patterns. Estimated dispersal distances for 41 BCI tree species (Muller-Landau et al. 2008) do show a significant negative relationship with abundance ($R^2 = 0.132$, P value = 0.0194; Suppl. Mat. Figure 4). Further, two separate studies have found that more abundant species have smaller NDD parameters (Comita et al. 2010, Mangan et al. 2010), although this is not a general result (Zhu et al. 2015). Another possibility, one not encompassed by our theoretical framework, is that more abundant species show stronger habitat associations, as such associations should produce more aggregated patterns. However, as stated earlier, these patterns should also be more persistent, contrary to observations.

The theoretical framework we utilize here is highly simplified; future work should explore more realistic and complex models incorporating size structure and temporal variation. Our models treat all individuals in a species as identical, whereas empirically there is large variation in size within species and associated variation in competitive ability, reproductive output, and survival probabilities. Analyses of spatially explicit models that include size or age classes (e.g., Murrell 2009) could evaluate the implications of this variation for spatiotemporal patterns in future developments of the theory. Our models also assume that underlying processes are constant in time, with constant reproductive rates, carrying capacities, etc. Yet empirical evidence shows that species abundances fluctuate more than would be expected based on demographic stochasticity alone, indicating important influences of environmental variability (Chisholm et al. 2014). At present, the effect of temporal environmental variability cannot be easily incorporated into this theory because death and birth events are considered uncorrelated with time (Ovaskainen and Cornell 2006b). Nonetheless, this topic could be explored through simulations.

CONCLUSIONS

The analysis of spatial point processes has been focused on discerning and quantifying spatial patterns of species distributions. Little attention has been devoted to understanding how these patterns evolve with time. Availability of multitemporal censuses permits the analysis of the dynamics of spatial patterns and recent theoretical advances in the study of spatially explicit models provide the foundation for such analyses.

Analysis of 221 abundant species in a forest dynamics plot revealed that the dynamics of spatial patterns deviate

in important and systematic ways from those expected under a univariate stochastic model, and thereby provides the important insight that more complex models that involve time delays implicitly or explicitly (through e.g., host-parasite dynamics) are needed to correctly represent spatial dynamics. This finding suggests that empirical analyses of NDD should examine performance not only in relation to current conspecific neighborhood densities, but also in relation to previous densities. Clearly an even greater advance in understanding could be obtained through explicit modeling of the interacting populations, e.g., of hosts and natural enemies.

In general, understanding of species level dynamics often requires observations over large areas and long temporal intervals. Aggregation and the persistence of spatial structures address two qualitatively different aspects of how species occupy space. The emergence of a general relationship between aggregation and persistence may enable inference of ecological properties even where spatial or temporal scales became limiting factors. It can also aid in the design of new observational studies and specifically in the choice of the temporal interval among censuses.

The simplified analytical and simulation models provide important insights into basic principles of spatially explicit problems, despite and at the same time because they lack of complexity to fully represent communities such as tropical forests. Future comparisons of these results with those from more complex and realistic models will help us to better connect them with data and to more confidently interpret empirical patterns.

ACKNOWLEDGMENTS

The BCI forest dynamics research project was founded by S.P. Hubbell and R.B. Foster and is now managed by R. Condit, S. Lao, and R. Perez under the Center for Tropical Forest Science and the Smithsonian Tropical Research in Panama. Numerous organizations have provided funding, principally the U.S. National Science Foundation, and hundreds of field workers have contributed. We thank E. G. Leigh, Jr., R. Chisholm, and anonymous reviewers for helpful comments.

LITERATURE CITED

- Allen, J. C., W. M. Schaffer, and D. Rosko. 1993. Chaos reduces species extinction by amplifying local population. *noiseNature* 364:229–232.
- Anderson-Teixeira, K., et al. 2014. CTFs-ForestGEO: a worldwide network monitoring forests in an era of global change. *Global Change Biology* 21:528–549.
- Bagchi, R., R. E. Gallery, S. Gripenberg, S. J. Gurr, L. Narayan, C. E. Addis, R. P. Freckleton, and O. T. Lewis. 2014. Pathogens and insect herbivores drive rainforest plant diversity and composition. *Nature* 506:85–88.
- Baldeck, C. A., et al. 2013. Habitat filtering across tree life stages in tropical forest communities. *Proceedings. Biological Sciences/The Royal Society* 280:20130548.
- Bartlett, M. 1964. The spectral analysis of two-dimensional point processes. *Biometrika* 51:299–311.
- Bolker, B., and S. Pacala. 1997. Using moment equations to understand stochastically driven spatial pattern formation in ecological systems. *Theoretical Population Biology* 52:179–197.

- Bolker, B., and S. Pacala. 1999. Spatial moment equations for plant competition: understanding spatial strategies and the advantages of short dispersal. *American Naturalist* 153:575–602.
- Bolker, B. M., S. W. Pacala, and S. A. Levin. 2000. Moment methods for ecological processes in continuous space. Pages 388–411 in U. Diekmann, R. Law, and J. A. J. Metz, editors. *The geometry of ecological interactions*. Cambridge University Press, Cambridge.
- Chisholm, R. A., R. Condit, et al. 2014. Temporal variability of forest communities: empirical estimates of population change in 4000 tree species. *Ecology Letters* 17:855–865.
- Comita, L., H. Muller-Landau, S. Aguilar, and S. Hubbell. 2010. Asymmetric density dependence shapes species abundances in a tropical tree community. *Science* 329:330–332.
- Condit, R., et al. 2000. Spatial patterns in the distribution of tropical tree species. *Science* 288:1414–1418.
- Condit, R., B. Engelbrecht, D. Pinob, R. Pérez, and B. L. Turner. 2013. Species distributions in response to individual soil nutrients and seasonal drought across a community of tropical trees. *Proceedings of the National Academy of Sciences of the United States of America* 110:5064–5068.
- Daley, D., and D. Vere-Jones. 2003. *An introduction to the theory of point processes, Volume I: elementary theory and methods*. Technometrics. Second edition. Springer-Verlag, New York.
- Detto, M., and H. C. Muller-Landau. 2013. Fitting ecological process models to spatial patterns using scalewise variances and moment equations. *American Naturalist* 181:E68–E82.
- Detto, M., H. C. Muller-Landau, J. Mascaro, and G. P. Asner. 2013. Hydrological networks and associated topographic variation as templates for the spatial organization of tropical forest vegetation. *PLoS ONE* 8:e76296.
- Flügge, A., S. Olhede, and D. Murrell. 2012. The memory of spatial patterns: changes in local abundance and aggregation in a tropical forest. *Ecology* 93:1540–1549.
- Gilbert, G. S., E. Howard, B. Ayala-Orozco, M. Bonilla-Moheno, J. Cummings, S. Langridge, I. M. Parker, J. Pasari, D. Schweizer, and S. Swope. 2010. Beyond the tropics: forest structure in a temperate forest mapped plot. *Journal of Vegetation Science* 21:388–405.
- Harms, K., S. Wright, O. Calderón, A. Hernandez, and E. Herre. 2000. Pervasive density-dependent recruitment enhances seedling diversity in a tropical forest. *Nature* 403:493–495.
- Harms, K. E., R. Condit, S. P. Hubbell, and R. B. Foster. 2001. Habitat associations of trees and shrubs in a 50-ha neotropical forest plot. *Journal of Ecology* 89:947–959.
- Harrison, R. D., S. Tan, J. B. Plotkin, F. Slik, M. Detto, T. Brenes, A. Itoh, and S. J. Davies. 2013. Consequences of defaunation for a tropical tree community. *Ecology Letters* 16:687–694.
- Holt, R. 1977. Predation, apparent competition, and the structure of prey communities. *Theoretical Population Biology* 12:197–229.
- Hubbell, S., R. Foster, and S. O'Brien. 1999. Light-gap disturbances, recruitment limitation, and tree diversity in a neotropical forest. *Science* 283:554–557.
- Lande, R., E. Steiner, and S. Bernt-Erick. 1999. Spatial scale of population synchrony: environmental correlation versus dispersal and density regulation. *American Naturalist* 154:271–281.
- Law, R., and U. Dieckmann. 2000. A dynamical system for neighborhoods in plant communities. *Ecology* 81:2137–2148.
- Law, R., J. Illian, D. F. R. P. Burslem, G. Gratzner, C. V. S. Gunatilleke, and I. A. U. N. Gunatilleke. 2009. Ecological information from spatial patterns of plants: insights from point process theory. *Journal of Ecology* 97:616–628.
- Lebrija-Trejos, E., S. Wright, A. Hernández, and P. Reich. 2014. Does relatedness matter? Phylogenetic density-dependent survival of seedlings in a tropical forest. *Ecology* 95:940–951.
- Losos, E., and E. G. J. Leigh, editors. 2004. *Tropical forest diversity and dynamism: findings from a large-scale plot network*. Chicago University Press, Chicago, Illinois, USA.
- Mangan, S. A., S. A. Schnitzer, E. a Herre, K. M. L. Mack, M. C. Valencia, E. I. Sanchez, and J. D. Bever. 2010. Negative plant-soil feedback predicts tree-species relative abundance in a tropical forest. *Nature* 466:752–755.
- Manrubia, S., and R. Solé. 1997. On forest spatial dynamics with gap formation. *Journal of Theoretical Biology* 187:159–164.
- Muller-Landau, H., S. Wright, O. Calderón, S. Hubbell, and R. Foster. 2002. Assessing recruitment limitation: concepts, methods and examples for tropical forest trees. Pages 653–667 in J. Levey, W. Silva, and M. Galett, editors. *Seed dispersal and frugivory: ecology, evolution and conservation*. CAB International, Oxfordshire, UK.
- Muller-Landau, H. C., S. J. Wright, O. Calderón, R. Condit, and S. P. Hubbell. 2008. Interspecific variation in primary seed dispersal in a tropical forest. *Journal of Ecology* 96:653–667.
- Murrell, D. J. 2009. On the emergent spatial structure of size-structured populations: when does self-thinning lead to a reduction in clustering? *Journal of Ecology* 97:256–266.
- Ovaskainen, O., and S. J. Cornell. 2006a. Asymptotically exact analysis of stochastic metapopulation dynamics with explicit spatial structure. *Theoretical Population Biology* 69:13–33.
- Ovaskainen, O., and S. J. Cornell. 2006b. Space and stochasticity in population dynamics. *Proceedings of the National Academy of Sciences of the United States of America* 103:12781–12786.
- Pacala, W. 1997. Dynamics of plant communities. Pages 532–555 in M. Crawley, editor. *Plant ecology*. Blackwell Science Ltd, Oxford.
- Seidler, T. G., and J. B. Plotkin. 2006. Seed dispersal and spatial pattern in tropical trees. *PLoS Biology* 4:e344.
- Tilman, D., R. May, C. Lehman, and M. Nowak. 1994. Habitat destruction and the extinction debt. *Nature* 371:65–66.
- Uriarte, M., S. Hubbell, R. John, R. Condit, and C. Canham. 2005. Neighborhood effects on sapling growth and survival in a neotropical forest and the ecological equivalence hypothesis. Pages 89–105 in D. F. R. P. Burslem, M. A. Pinard, and S. Hartley, editors. *Biotic interactions in the tropics: their role in the maintenance of species diversity*. Cambridge University Press, Cambridge.
- Wiegand, T., and K. Moloney. 2013. *Handbook of spatial point-pattern analysis in ecology*. CRC Press, Boca Rato.
- Zhu, K., C. W. Woodall, J. V. D. Monteiro, and J. S. Clark. 2015. Prevalence and strength of density-dependent tree recruitment. *Ecology* 96:2319–2327.

SUPPORTING INFORMATION

Additional supporting information may be found in the online version of this article at <http://onlinelibrary.wiley.com/doi/10.1890/15-1505.1/supinfo>